Deletion of Skeletal Muscle SOCS3 Prevents Insulin Resistance in Obesity

Sebastian Beck Jorgensen,[1,2] Hayley M. O'Neill,[1,3] Lykke Sylow,[4] Jane Honeyman,[1] Kimberly A. Hewitt,[1] Rengasamy Palanivel,[3] Morgan D. Fullerton,[3] Lisa Öberg,[5] Anudharan Balendran,[5] Sandra Galic,[1] Chris van der Poel,[6] Ian A. Trounce,[7] Gordon S. Lynch,[6] Jonathan D. Schertzer,[3] and Gregory R. Steinberg[1,3]

Obesity is associated with chronic low-grade inflammation that contributes to defects in energy metabolism and insulin resistance. Suppressor of cytokine signaling (SOCS)-3 expression is increased in skeletal muscle of obese humans. SOCS3 inhibits leptin signaling in the hypothalamus and insulin signal transduction in adipose tissue and the liver. Skeletal muscle is an important tissue for controlling energy expenditure and whole-body insulin sensitivity; however, the physiological importance of SOCS3 in this tissue has not been examined. Therefore, we generated mice that had SOCS3 specifically deleted in skeletal muscle (SOCS MKO). The SOCS3 MKO mice had normal muscle development, body mass, adiposity, appetite, and energy expenditure compared with wild-type (WT) littermates. Despite similar degrees of obesity when fed a high-fat diet, SOCS3 MKO mice were protected against the development of hyperinsulinemia and insulin resistance because of enhanced skeletal muscle insulin receptor substrate 1 (IRS1) and Akt phosphorylation that resulted in increased skeletal muscle glucose uptake. These data indicate that skeletal muscle SOCS3 does not play a critical role in regulating muscle development or energy expenditure, but it is an important contributing factor for inhibiting insulin sensitivity in obesity. Therapies aimed at inhibiting SOCS3 in skeletal muscle may be effective in reversing obesity-related glucose intolerance and insulin resistance. ***Diabetes*** **62:56–64, 2013**

Obesity is associated with a chronic low-grade inflammatory response that induces defects in energy balance, insulin sensitivity, and lipid metabolism (1). The suppressor of cytokine signaling (SOCS) family of proteins (SOCS1–7), which bind via their SH2 domains to tyrosine phosphorylation sites on cytokine receptors, inhibit inflammatory signal transduction. In obesity, consistent with increases in inflammation, SOCS3 is upregulated in the hypothalamus (2), adipose tissue (3), and liver (4,5). SOCS3 expression is also increased in human and rodent skeletal muscle with obesity (6,7).

Skeletal muscle is an important tissue contributing to basal metabolic rate and control of whole-body insulin sensitivity. A recent study has shown that the overexpression of SOCS3 in skeletal muscle by ~150-fold disrupts calcineurin signaling, resulting in defects in muscle sarcoplasmic reticulum and mitochondria (8). As a result of impaired muscle development, transgenic SOCS3-overexpressing mice had reduced ambulatory activity levels. Although these data suggest a potentially intriguing role for SOCS3 in regulating muscle function, a major caveat of these studies involving the overexpression of SOCS3 is that, in the absence of overt inflammation, SOCS3 expression in muscle is low (9). SOCS3 also may play an important role in regulating energy balance because it inhibits leptin activation of Y985 within the leptin receptor (10,11). SOCS3 heterozygous mice (12) or those with SOCS3 deleted in hypothalamic neurons (13) have reduced appetite and are protected from development of diet-induced obesity attributable to enhanced hypothalamic leptin sensitivity within proopiomelanocortin-expressing neurons (11). Like the hypothalamus, we have shown that skeletal muscle also becomes resistant to leptin in obesity (14,15), which is characterized by an impaired ability of leptin to increase fatty acid oxidation via the AMP-activated protein kinase (AMPK) (16). In cultured muscle cells, the overexpression of SOCS3 inhibits leptin activation of AMPK and fatty acid oxidation (17). However, because leptin also activates AMPK in skeletal muscle via hypothalamic circuits (18), it is unknown whether physiological increases in SOCS3 expression in obesity (two- to threefold) may be of biological importance for regulating muscle function and energy balance.

SOCS3 is an important negative regulator of insulin signaling (19). Genetic deletion of SOCS3 from mouse liver results in enhanced insulin signaling because of increased insulin receptor substrate 1 (IRS1) phosphorylation (20,21). However, when mice are fed a high-fat diet (HFD), the enhanced liver insulin sensitivity paradoxically promotes liver lipogenesis, exacerbating the development of nonalcoholic fatty liver disease, systemic inflammation, and the onset of obesity (21). These data, which are in contrast to transient partial reductions in SOCS3 expression using small interfering RNA (5,22), suggest that chronic inhibition of SOCS3 in the liver is not an appropriate treatment for insulin resistance in obesity. In skeletal muscle, SOCS3 has been shown to coimmunoprecipitate with both the insulin receptor (IR) and IRS1 (23); however, in contrast to reports in adipose tissue (24) and liver (5), the overexpression of

From the [1]St. Vincent's Institute of Medical Research and Department of Medicine, University of Melbourne, Fitzroy, Victoria, Australia; the [2]Diabetes Research Unit, Novo Nordisk A/S, Maaloev, Denmark; the [3]McMaster University, Department of Medicine and Biochemistry and Biomedical Sciences, Hamilton, Ontario, Canada; the [4]Department of Exercise and Sport Sciences, Section of Human Physiology, Molecular Physiology Group and Copenhagen Muscle Research Centre, Copenhagen, Denmark; the [5]AstraZeneca R&D Mölndal, Mölndal, Sweden; the [6]University of Melbourne, Basic and Clinical Myology Laboratory, Department of Physiology, Parkville, Victoria, Australia; and the [7]Centre for Eye Research Australia, University of Melbourne, Royal Victorian Eye and Ear Hospital, Melbourne, Victoria, Australia.

Corresponding author: Gregory R. Steinberg, gsteinberg@mcamster.ca.

Received 10 April 2012 and accepted 21 June 2012.

DOI: 10.2337/db12-0443

This article contains Supplementary Data online at http://diabetes.diabetesjournals.org/lookup/suppl/doi:10.2337/db12-0443/-/DC1.

SOCS3 in skeletal muscle is not associated with reduced IRS1 signaling or the development of insulin resistance (8).

Given the importance of skeletal muscle in the regulation of energy metabolism and insulin sensitivity, we generated mice with muscle-specific deletion of SOCS3 (SOCS3 MKO). We demonstrate that deletion of SOCS3 in muscle does not alter muscle development, body mass, adiposity, or energy expenditure, but it causes substantial protection against the development of obesity-induced hyperinsulinemia and hyperglycemia attributable to enhanced skeletal muscle IRS1 phosphorylation and glucose uptake.

RESEARCH DESIGN AND METHODS

Animal experimental procedures. All procedures were approved by St. Vincent's Hospital and McMaster University Animal Ethics Committees. The SOCS3 MKO mice were generated by crossing SOCS3 floxed mice (generated on a C57Bl6 background [25]) with mice expressing Cre-recombinase under the control of the muscle creatine kinase promoter (26) that had been backcrossed to a C57Bl6 background for at least 10 generations. All mice were maintained on a 12-h light/dark cycle with lights on at 0700 h. At 6 weeks, SOCS3 MKO or wild-type (WT) littermates were randomly assigned to one of two diets, a standard (control) rodent chow diet containing 17% of calories from fat (Diet 8640; Harlan Teklad, Madison, WI) or HFD containing 45% calories from fat (Diet SF04-027; Specialty Feeds, Glen Forrest, West Adelaide, Australia). Body mass was monitored weekly. Metabolic rate and activity levels were measured using a Columbus Instruments Laboratory Animal Monitoring System over 72 h after mice had been on their respective diets for 11 weeks as described (27,28). Leptin/saline injection experiments were conducted in a separate cohort of HFD-fed mice that were acclimatized to the metabolic cages and daily saline injections at 0700 h for 4 days. On day 1 of the experiment, mice were injected at 0700 h with saline, followed by leptin (3 mg/kg) 24 h later as described (29). Glucose (1 g/kg D-glucose) and insulin (0.5 units/kg) tolerance tests were performed 6 h after removal of food as described (21,30). Treadmill running capacity testing was completed in ad libitum chow-fed mice after 2 days of acclimatization as described (28). Tibialis anterior muscle function and cross-sectional area were assessed as described previously (31). For determination of insulin signaling, control-fed and HFD-fed SOCS3 MKO mice that were fasted overnight were anesthetized and injected with a bolus of insulin (0.5 units/kg) via the descending branch of the inferior vena cava and tissues collected 5 min later as described (21). Basal and insulin-stimulated (100 nmol/L) 2-deoxyglucose uptake was determined in isolated extensor digitorium longus muscles isolated from mice fed ad libitum as described (32). Basal and leptin-stimulated (10 μg/mL) palmitate oxidation were determined in isolated soleus muscles from mice fed ad libitum as described (14).

In vivo glucose uptake. ^{18}F-Fluorodeoxyglucose (FDG) was synthesized by nucleophilic substitution method using an FDG synthesizing instrument (GE Healthcare, Milwaukee, WI) and a cyclotron (Siemans 20–30 gb). Positron emission tomography (PET) was performed using an advance scanner (Philip Mosaic PET Scanner). After fasting for 8 h, mice were restrained and injected with 0.9% saline (control) or insulin (0.5 units/kg, the same dose used in the insulin tolerance test diluted in 0.9% saline for 5 min, and then received intravenous administration of FDG (10.8 ± 1.2 MBq; Hamilton Health Sciences and McMaster University). All mice underwent small-animal PET and microcomputed tomography (CT; γ Medica-Ideas Xspect System, Northridge, CA), and whole-body PET images were acquired 30 min later. After injection, the mice were maintained under conscious conditions and warmed using a heating pad. Mice were imaged at exactly 30 min after injection using an acquisition time of 15 min for PET and followed by CT for 5 min. Images were reconstructed using 3D-RAMLA algorithm, with no attenuation correction and no correction for partial-volume effects of the tomograph. Quantification was performed by region-of-interest analysis using AMIRA Research Workplace software and FDG tissues uptake was calculated using the mean value of standardized uptake units as described (33). Body composition was calculated from the CT image as recently described (27)

Quantitative RT-PCR. RNA from tibialis anterior or mixed gastrocnemius muscle (as indicated) was isolated using the RNeasy mini kit (Qiagen, Doncaster, Australia), reverse-transcribed using the Thermoscript RT-PCR system (Invitrogen, Mt Waverley, Australia), and analyzed via quantitative RT-PCR on the Rotorgene 3000 (Corbett Research, Sydney, Australia) using SOCS3 primers and normalized using 18S ribosomal RNA as described (21,34).

Protein analysis. Frozen gastrocnemius muscles (~50 mg) were prepared in homogenization buffer supplemented with protease and phosphatase inhibitors, and immunoblotting was conducted using antibodies as described (32,34,35).

Mitochondrial enzyme activities. Mitochondria were isolated from fresh (not frozen) gastrocnemius muscle by differential centrifugation, and activities of oxidative phosphorylation complexes were measured on sonicated samples using spectrophotometric assays as previously described (36). Briefly, NADH–ubiquinone oxidoreductase (complex I) activity was measured as the rotenone-sensitive oxidation of NADH using decylubiquinone as electron acceptor; ubiquinol–cytochrome c oxidoreductase (complex III, antimycin-sensitive activity) was measured using reduced decylubiquinone as an electron donor and cytochrome c as an electron acceptor; cytochrome c oxidase (complex IV) activity was measured using reduced cytochrome c as an electron donor (35).

Plasma metabolite, hormones, and cytokines. Whole blood was spun at 7,000*g* for 5 min at 4°C, and the serum was removed. Plasma hormone and cytokines were assessed using a Lincoplex mouse serum adipokine panel (35).

Electron microscopy. Transmission electron microscopy was used to determine tibialis anterior muscle and mitochondrial morphology and distribution as recently described (28).

Gene expression profiling. Tibialis anterior muscle from WT and SOCS3 MKO mice fed a chow diet or an HFD for 12 weeks (n = 8 per group) were dissected after a 6 h fast at the start of the light cycle and snap-frozen. RNA extraction and microarray analysis using Affymetrix Mouse Exon 1.0 ST arrays were performed by Almac Diagnostics (Craigavon, Northern Ireland). Total RNA was extracted using TriZol, cDNA was prepared using NuGENs WT-Ovation Pico RNA Amplification Kit, and sense transcript cDNA was prepared using NuGENs WT-Ovation Exon Module. Fragmentation, labeling, and hybridization to arrays were performed with NuGENs FL-Ovation cDNA Biotin Module V2. The arrays were stained, washed, and scanned in accordance to the Affymetrix GeneChip whole-transcript sense target labeling assay manual. Raw data from the scanned arrays were further processed and analyzed using ArrayStudio (Omicsoft Corporation, Cary, NC). Data were normalized using the Robust Multiarray Average method. One array (from the WT chow-fed group) was identified as abnormal in the quality-control process and excluded from further analysis. Differential expression was assessed on the core transcript (gene) level using a general linear model (model: ~type+diet+type: diet) with an adjustment for multiple test correction (Benjamini-Hochberg). Significance was accepted at adjusted $P \leq 0.05$.

Calculations and statistical analysis. All data are reported as mean ± SE. Results were analyzed by t test or ANOVA procedures and a Bonferroni post hoc test when appropriate. Significance was accepted at $P \leq 0.05$.

RESULTS

SOCS3 MKO mice have normal muscle development. A bolus of lipopolysaccharide (2 mg/kg) dramatically increased SOCS3 mRNA (2 h after injection) in WT mice, and this effect was markedly blunted in muscle and heart but not other tissues (liver, epididymal white adipose, or hypothalamus) of SOCS3 MKO mice (Supplementary Fig. 1*A*). SOCS3 mRNA detected in muscle of SOCS3 MKO mice was most likely attributable to contamination from other tissues. Consistent with the well-documented efficiency of the muscle creatine kinase promoter (26), SOCS3 protein expression was not detected in soleus muscle and was dramatically reduced in the heart of SOCS3 MKO mice after a bolus of lipopolysaccharide (Supplementary Fig. 1*B*). Given the reported role of SOCS3 in regulating muscle fiber development (8,37), we examined muscle cross-sectional area and used electron microscopy imaging to explore intracellular muscle morphology. There were no differences in muscle fiber size and structure or mitochondrial size between genotypes (Fig. 1*A* and *B*). We also tested exercise capacity as well as muscle fatigability and capacity to generate force and found that these parameters were all comparable between genotypes (Supplementary Table 1 and Fig. 1*C* and *D*). Therefore, in contrast to the transgenic overexpression of SOCS3 (8,37), endogenous levels of skeletal muscle SOCS3 are not essential for regulating muscle development or performance.

SOCS3 MKO mice are not protected from diet-induced obesity. The overexpression of SOCS3 in skeletal muscle has been shown to lead to HFD-induced obesity (8) and suppress leptin activation of STAT3, AMPK, and

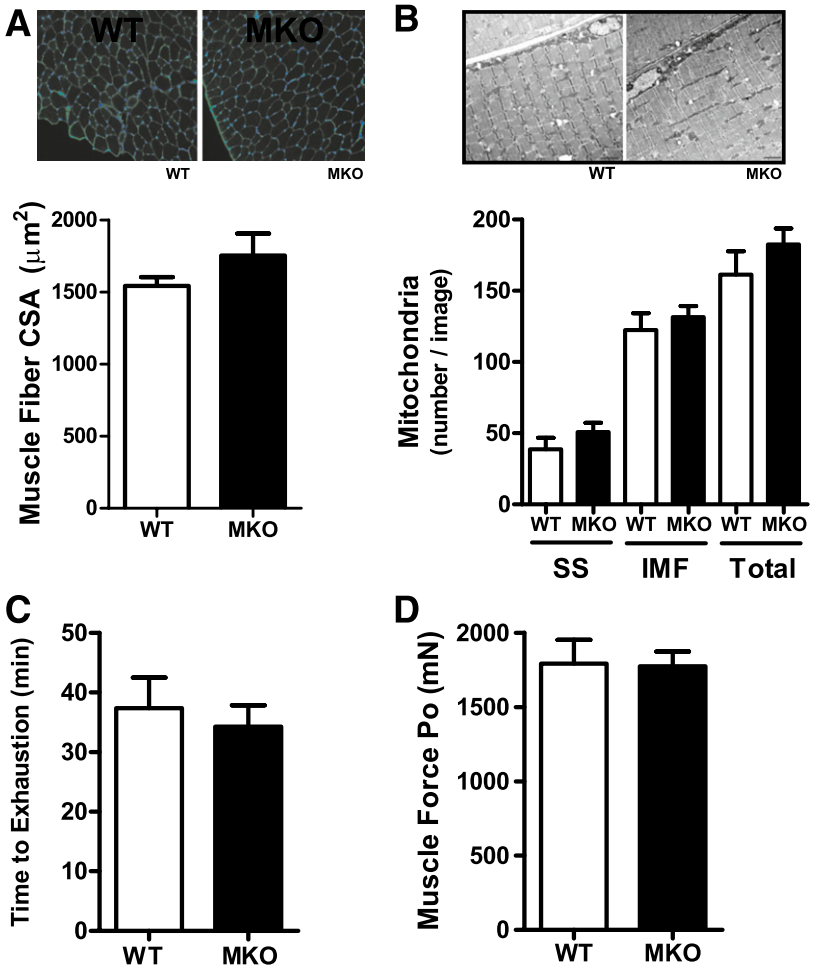

FIG. 1. Muscle-specific deletion of SOCS3 does not alter muscle development or performance. *A*: Tibialis anterior muscle histology (*top*) and quantification of muscle fiber cross-sectional area (CSA) (n = 3). *B*: Electron microscopy image (*top*) and quantification of mitochondrial content (*right*) in subsarcolemmal (SS) and intramyofibrillar (IMF) regions of tibialis anterior muscle (n = 3, scale bar = 2 μm, total = SS+IMF). *C*: Treadmill running capacity. *D*: Peak absolute force of tibialis anterior muscles (n = 7–10). All data were obtained from 10-week-old chow-fed male WT and SOCS3 MKO mice. (A high-quality color representation of this figure is available in the online issue.)

fatty acid oxidation (15,17). We therefore hypothesized that SOCS3 MKO mice would not develop HFD-induced obesity. In chow-fed mice, SOCS3 expression in muscle was at the limits of detection of our assay in both WT and SOCS3 MKO mice (Fig. 2*A*). Obesity increases SOCS3 expression (6,7) and, as anticipated, SOCS3 expression was increased by approximately twofold in muscle from WT but not SOCS3 MKO mice after 12 weeks of an HFD (Fig. 2*A*). SOCS1, which is homologous to SOCS3 and also regulates insulin sensitivity, was not altered by diet or genotype (Supplementary Table 2). There was no difference in body mass or adiposity when mice were fed a chow diet (Fig. 2*B* and *C*) and, as anticipated, the HFD induced substantial increases in these parameters, but there was no difference between genotypes (Fig. 2*B* and *C*). Female SOCS3 MKO mice also had similar body mass as WT littermates (Supplementary Fig. 2*A*).

Increased glucose tolerance, insulin sensitivity, and metabolic flexibility in obese SOCS3 MKO mice. Fasting blood glucose was increased by the HFD and was modestly lower in SOCS3 MKO mice (Fig. 2*D*). Importantly, SOCS3 MKO mice had lower serum insulin irrespective of diet (Fig. 2*E*). When fed the chow diet, there were no differences between genotypes in regard to

TABLE 1
Oxygen consumption (V_{O_2}), spontaneous activity levels, and food intake in HFD-fed WT and SOCS3 MKO mice

	WT		SOCS3 MKO	
	Dark	Light	Dark	Light
V_{O_2} (mL/kg/h)	2,993 ± 110	2,458 ± 103*	3,097 ± 87	2,501 ± 66*
Activity (beam breaks/12 h)	37,742 ± 2,208	4,690 ± 794*	36,438 ± 1,880	4,949 ± 910*
Food intake (g/12 h)	1.46 ± 0.14	0.81 ± 0.04*	1.60 ± 0.21	0.71 ± 0.10*

Data are means ± SE over 12-h dark (1900–0700 h) and light (0700–1900 h) cycles. n = 8. V_{O_2}, oxygen consumption. *$P \leq 0.05$ vs. dark, same genotype.

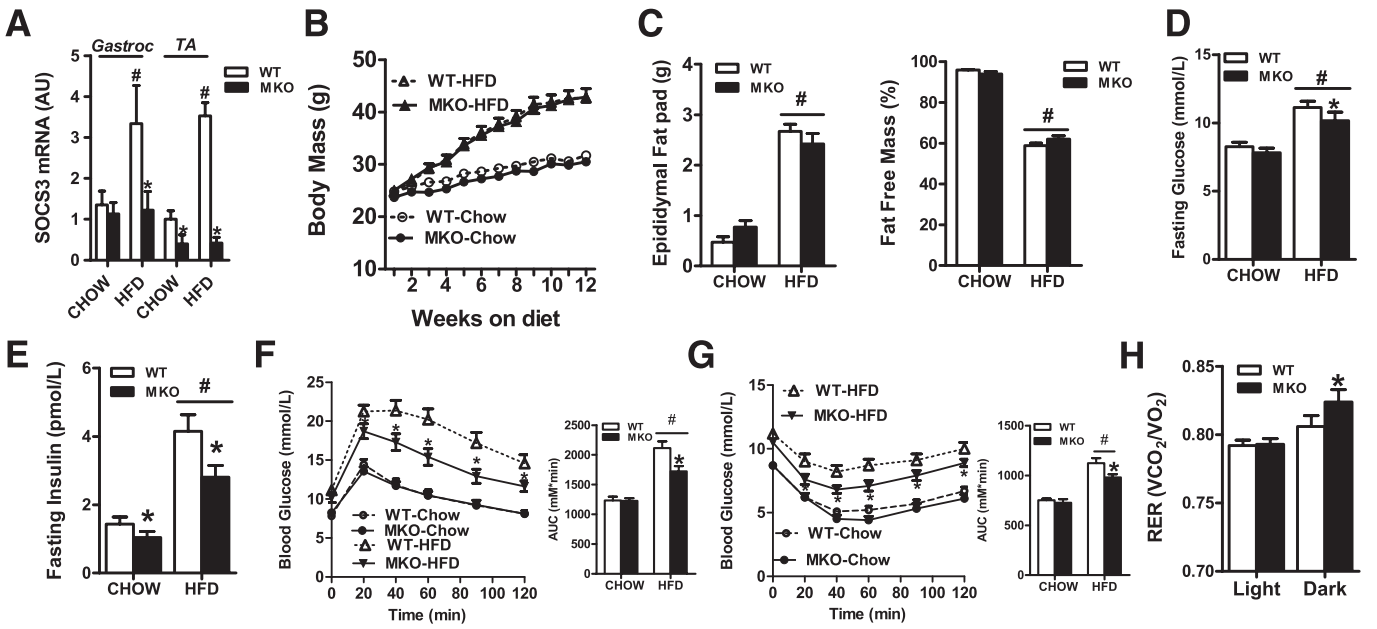

FIG. 2. SOCS3 MKO mice are protected from insulin resistance and glucose intolerance despite similar body mass. *A*: Mixed gastrocnemius (Gastroc) and tibialis anterior (TA) muscle SOCS3 mRNA expression after 12 weeks of either a control chow diet or an HFD. *B*: Growth curves in WT and SOCS3 MKO mice fed either a chow diet or an HFD for 12 weeks. *C*: Epididymal fat pad weight (*left*) and fat-free mass (*right*) in WT and SOCS3 MKO mice fed either a chow diet or an HFD for 12 weeks. Blood glucose (*D*) and serum insulin (*E*) after a 6-h fast in WT and SOCS3 MKO mice fed either a chow diet or an HFD for 12 weeks are shown. Glucose tolerance (*F*) and insulin sensitivity (*G*) after a 6-h fast in WT and SOCS3 MKO mice fed either a chow diet or an HFD for 12 weeks are shown (*inset* area under the curve [AUC]). *H*: Respiratory exchange ratio (RER) in WT and SOCS3 MKO mice fed either a chow diet or an HFD for 11 weeks. Data are from male mice and are shown as mean ± SE, n = 7–10. #$P < 0.05$ relative to chow control. *$P \leq 0.05$ relative to WT.

glucose tolerance and insulin sensitivity (Fig. 2*F* and *G*). As expected, the HFD impaired whole-body glucose tolerance and insulin sensitivity in WT mice, but SOCS3 MKO mice had marked improvements in these parameters (Fig. 2*F* and *G*). Similar observations were made in female SOCS3 MKO mice (Supplementary Fig. 2*B* and *C*). Thus, deletion of skeletal muscle SOCS3 protects mice from obesity-induced glucose intolerance and insulin resistance

To assess whether improvements in glucose homeostasis in HFD-fed SOCS3 MKO mice were related to alterations in whole-body energy expenditure, we assessed oxygen consumption (V_{O_2}), substrate utilization, habitual physical activity, and the respiratory exchange ratio. There were no differences in oxygen utilization, activity levels, or food intake (Table 1). However, during the dark cycle, SOCS3 MKO mice had a higher respiratory exchange ratio, indicating greater carbohydrate oxidation during feeding (Fig. 2*H*), a finding that is indicative of enhanced metabolic flexibility and improved insulin sensitivity (38).

SOCS3 MKO mice have normal muscle AMPK, mitochondrial content, and triglyceride. To assess potential mechanisms for the improvements in whole-body insulin sensitivity and glucose tolerance, we measured serum adipokines/cytokines, which are known to increase SOCS3 expression. Consistent with increased adiposity in HFD mice, we found that serum tumor necrosis factor-α and resistin were elevated by ~35% and 220%, respectively, but there were no differences between genotypes (Table 2). Serum interleukin-6 and nonesterified fatty acids were not affected by either diet or genotype

TABLE 2
Serum adipokines, nonesterified fatty acids, and hyperinsulemic-euglycemic clamp parameters in WT and SOCS3 MKO mice fed a chow diet or an HFD

	Chow		HFD	
	WT	SOCS3 MKO	WT	SOCS3 MKO
Leptin (ng/mL)	8.55 ± 0.90	1.81 ± 0.41*	14.76 ± 1.45†	13.8 ± 0.85†
TNFα (pg/mL)	3.17 ± 0.20	2.98 ± 0.37	4.53 ± 0.82†	3.96 ± 0.56†
IL-6 (pg/mL)	3.46 ± 0.86	3.39 ± 1.01	3.61 ± 0.75	5.08 ± 0.042
Resistin (ng/mL)	1.3 ± 0.2	1.2 ± 0.17	4.2 ± 0.59†	4.1 ± 0.39†
NEFA (mmol/L)	1.25 ± 0.18	1.26 ± 0.12	1.24 ± 0.08	1.28 ± 0.06
Preclamp glucose (mmol/L)	5.7 ± 0.3	5.5 ± 0.6	6.3 ± 0.50†	6.1 ± 0.50†
Clamp glucose (mmol/L)	5.9 ± 0.1	5.8 ± 0.1	6.0 ± 0.13	5.8 ± 0.12
Basal glucose disposal rate (mg/kg/min)	33.5 ± 4.5	40.5 ± 5.7	26.7 ± 2.5†	30.4 ± 1.4†
Suppression hepatic glucose output (%)	92.7 ± 1.3	91.2 ± 2.1	84.1 ± 4.9†	84.6 ± 3.04†

Data are means ± SE for n = 6–8. IL, interleukin; NEFA, nonesterified fatty acid; TNF, tumor necrosis factor. *$P < 0.05$ vs. WT from same dietary condition. †$P \leq 0.05$ vs. chow, same genotype.

(Table 2). Surprisingly, despite similar adiposity, serum leptin in chow-fed but not HFD-fed SOCS3 MKO mice was ~80% lower compared with WT, suggesting that a potential myokine whose secretion is altered in chow-fed SOCS3 MKO mice may be important for regulating leptin production (Table 2). The in vitro leptin treatment of muscle increases skeletal muscle fatty acid oxidation in lean, but not obese, rodents and humans (17,18,34). Consistent with these findings, we found that leptin increased fatty acid oxidation in chow-fed but not HFD-fed soleus muscle from WT mice (Fig. 3*A*). However, in contrast to WT mice, leptin-stimulated fatty acid oxidation was maintained in muscles from HFD-fed SOCS MKO mice (Fig. 3*A*). To examine whether HFD-fed SOCS3 MKO mice also had enhanced sensitivity to leptin in vivo, mice were placed in metabolic cages and injected with saline or leptin at the start of the light cycle (0700 h). In contrast to our in vitro findings, leptin modestly reduced respiratory exchange ratio, indicating an increase in fatty acid oxidation to a similar degree in both WT and SOCS3 MKO mice (Fig. 3*B*). Food intake also was modestly reduced by ~10% in both genotypes (Fig. 3*C*). We subsequently examined phosphorylation of STAT3 Y705, AMPK T172, and its downstream substrate acetyl-CoA carboxylase S212 and found that they were not altered by either genotype or diet (Fig. 3*D*). These data suggest that leptin increases whole-body rates of fatty acid oxidation through mechanisms independent of skeletal muscle SOCS3, potentially involving increases in adipose tissue lipolysis (39). Because AMPK (40,41) and leptin (42) are important for regulating muscle mitochondrial content, we measured a number of mitochondrial markers and found that they also were not different between genotypes with the exception of complex IV activity, which was increased in chow-fed SOCS3 MKO mice (Fig. 3*E* and *F*). Consistent with normal levels of muscle AMPK and mitochondrial content, we found that muscle triglyceride while increased severalfold with the HFD was not different between WT and SOCS3 MKO mice (Fig. 3*G*). Taken together, this suggests that improved insulin sensitivity in SOCS3 MKO mice is not attributable to alterations in skeletal muscle AMPK.

SOCS3 MKO mice have enhanced skeletal muscle insulin sensitivity. To determine the tissues that contribute to the improved whole-body insulin sensitivity of SOCS3 MKO mice, we performed hyperinsulinemic-euglycemic clamps. Serum glucose concentrations before and during the clamp were similar between WT and SOCS3 MKO mice (Table 2). Under chow-fed conditions, we detected no differences in the glucose infusion rate (Fig. 4*A*), glucose disposal rate (Fig. 4*B*), or hepatic glucose production (Fig. 4*C*) between WT and SOCS3 MKO mice. As anticipated, the HFD caused insulin resistance evinced by suppression in both the glucose infusion rate and the glucose disposal rate in WT mice, but this effect was blunted in the HFD-fed SOCS3 MKO mice (Fig. 4*A* and *B*). There were no changes in hepatic glucose production or insulin suppression of hepatic glucose production between genotypes (Fig. 4*C* and Table 2). These data indicate that deletion of SOCS3 from skeletal muscle improves whole-body insulin sensitivity because of enhanced glucose disposal.

To examine if an increase in muscle insulin-stimulated glucose uptake was responsible for the enhanced glucose disposal in HFD-fed SOCS3 MKO mice, we conducted PET imaging in mice injected with insulin (0.5 units/kg) and FDG. FDG uptake was comparable between WT and SOCS3 MKO epididymal white adipose, liver, heart ($P = 0.12$), kidney, and brain (Supplementary Table 3), but we found that the gastrocnemius muscle of SOCS3 MKO mice accumulated ~30% more FDG than WT littermates (Fig. 4*D*). To determine whether improved insulin sensitivity in obese SOCS3 MKO animals was attributable to intrinsic changes in the muscle and not attributable to a combination of insulin and potentially other circulating factors, we measured insulin-stimulated 2-deoxyglucose uptake in isolated muscles. Insulin

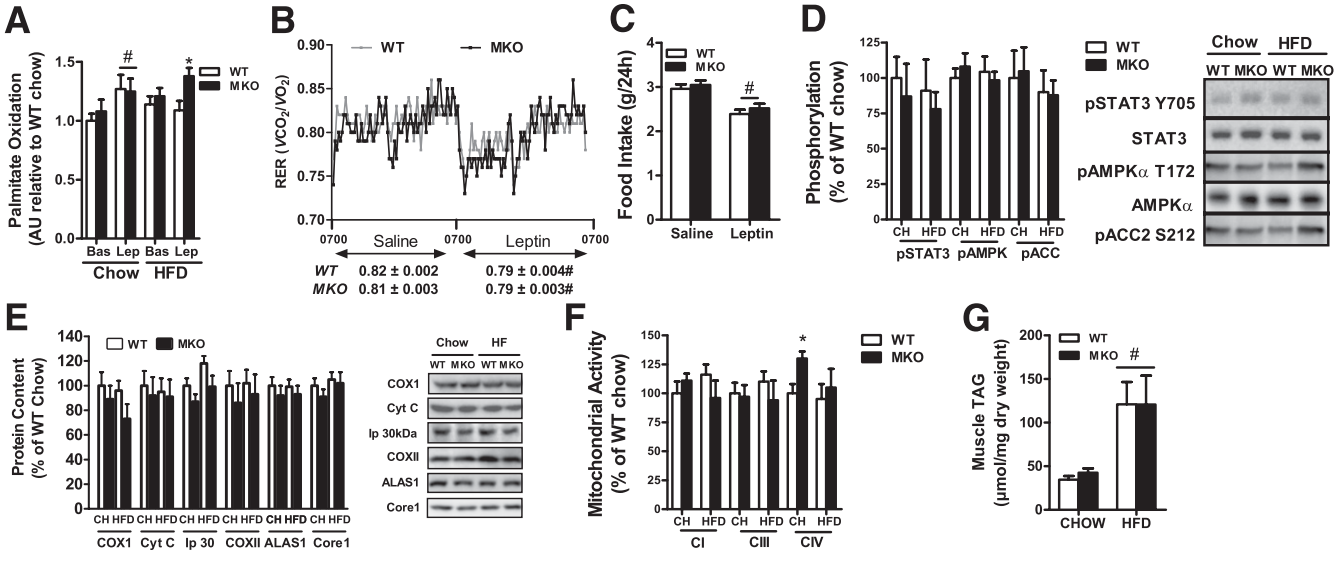

FIG. 3. Ex vivo, but not in vivo, skeletal muscle leptin sensitivity is improved in obese SOCS3 MKO mice. *A*: Soleus muscle palmitate oxidation from chow-fed or HFD-fed WT and SOCS3 MKO mice under basal conditions or with leptin (n = 6–9). Respiratory exchange ratio (RER) (*B*) and food intake (*C*) in WT and SOCS3 MKO mice fed an HFD injected with either saline or leptin (n = 6–8) are shown. Gastrocnemius muscle (*D*) STAT3 Y705, AMPK T172, and acetyl-CoA carboxylase (ACC2) S212 phosphorylation in male WT and SOCS3 MKO mice fed a chow diet or an HFD for 12 weeks are shown. Gastrocnemius muscle mitochondrial protein expression (*E*) and activity (*F*) from male WT and SOCS3 MKO mice fed a chow diet or HFD for 12 weeks (n = 6–8) are shown. *G*: Gastrocnemius muscle triacylglycerol (TAG) from male WT and SOCS3 MKO mice fed a chow diet or an HFD for 12 weeks (n = 6–8). Data are mean ± SE. *$P \leq 0.05$ relative to WT. #$P < 0.05$ relative to basal, saline, or chow conditions.

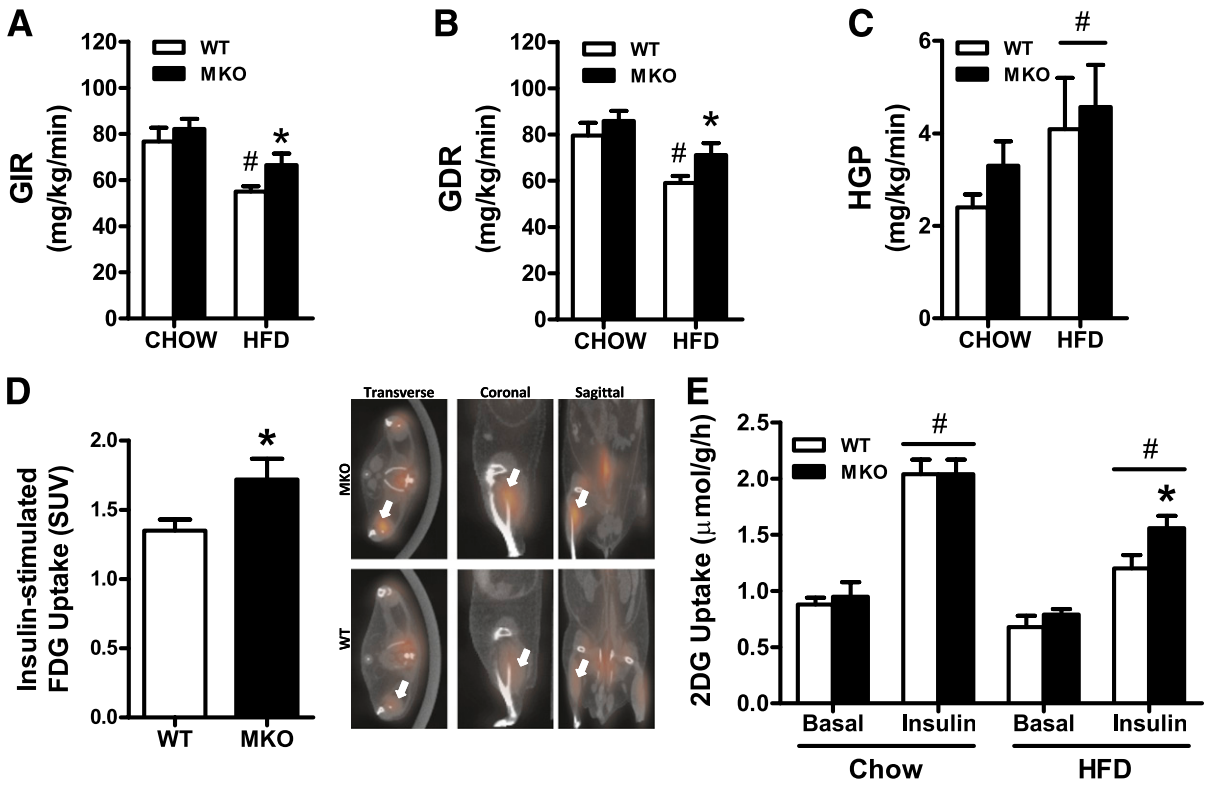

FIG. 4. Improved insulin sensitivity in HFD-fed SOCS3 MKO mice is attributable to enhanced insulin-stimulated glucose uptake into muscle. Hyperinsulinemic-euglycemic clamp results for insulin-stimulated glucose infusion rate (GIR) (*A*), glucose disposal rate (GDR) (*B*), and hepatic glucose production (HGP) (*C*) in female WT and SOCS3 MKO mice fed a chow diet or an HFD for 12 weeks are shown. *D*: Insulin-stimulated ^{18}F-Flourodeoxyglucose (FDG) uptake into skeletal muscle of male SOCS3 MKO mice fed an HFD for 12 weeks. *E*: Basal and insulin-stimulated 2-deoxyglucose (2DG) uptake into isolated extensor digitorium longus muscles from male WT and SOCS3 MKO mice fed a chow diet or HFD for 12 weeks. Data are mean ± SE, n = 7–10. #$P \leq 0.05$ relative to chow and/or basal control. *$P \leq 0.05$ relative to WT. (A high-quality color representation of this figure is available in the online issue.)

increased 2-deoxyglucose uptake by ~100% in isolated extensor digitorium longus muscle from chow-fed WT and SOCS3 MKO mice, and although the HFD suppressed this effect, muscles from SOCS3 MKO were more insulin-sensitive compared with WT littermates (Fig. 4*E*). This demonstrates that the deletion of skeletal muscle SOCS3 directly improves skeletal muscle insulin sensitivity in obesity.

Skeletal muscle SOCS3 inhibits IRS1 tyrosine phosphorylation. To elucidate potential mechanisms for the improved skeletal muscle insulin sensitivity in HFD-fed SOCS3 MKO mice, we performed a genome-wide expression analysis. In this analysis we found no differentially expressed genes between the WT and the SOCS3 MKO mice fed either a chow diet or an HFD (Fig. 5*A*). In contrast, 2,406 genes were differentially expressed as a consequence of diet (Fig. 5*A*). To further assess potential mechanisms, we measured total expression and phosphorylation of insulin signaling proteins. We found that IR, IRS1, and Akt expression were unaltered by SOCS3 deficiency (Fig. 5*B*). There was no difference in IR tyrosine phosphorylation between WT and SOCS3 MKO mice (Fig. 5*C*). However, the IRS1-associated P85 subunit of phosphatidylinositol (PI)-3 kinase was increased in HFD-fed SOCS3 MKO mice after insulin treatment (Fig. 5*D*). Similarly, insulin-stimulated Akt T308 and S473 phosphorylation were increased in SOCS3 MKO mice (Fig. 5*E*). These data demonstrate that skeletal muscle SOCS3 inhibits activating phosphorylation of IRS1 without altering global gene expression or the total protein expression of insulin signaling proteins.

DISCUSSION

Insulin resistance associated with obesity is a well-established forerunner for the development of type 2 diabetes and has been linked to both ectopic lipid accumulation (43) and low-grade chronic inflammation (44). Studies in hepatocytes and adipocytes have shown that overexpression of SOCS3 antagonizes proximal insulin signaling (3–5,24,45,46). However, surprisingly, when SOCS3 is genetically deleted from the liver, it propagates the development of obesity and fatty liver disease (20,21). These studies highlighted the need to investigate the role of endogenous levels of SOCS3 under physiological conditions such as obesity. Given that SOCS3 is elevated in skeletal muscle with obesity, and that skeletal muscle plays a major role in controlling energy expenditure and glucose homeostasis, we generated mice with muscle-specific deletion of SOCS3. The SOCS3 MKO mice did not express any major phenotypic abnormalities as assessed by growth and survival, organ weights, food intake, energy expenditure, or habitual physical activity levels. We specifically addressed muscle function and found that skeletal muscles from SOCS3 MKO mice had normal morphology and function.

SOCS3 whole-body heterozygous mice are protected against the development of obesity (12). The leptin receptor is expressed in skeletal muscle (47) and high levels of leptin

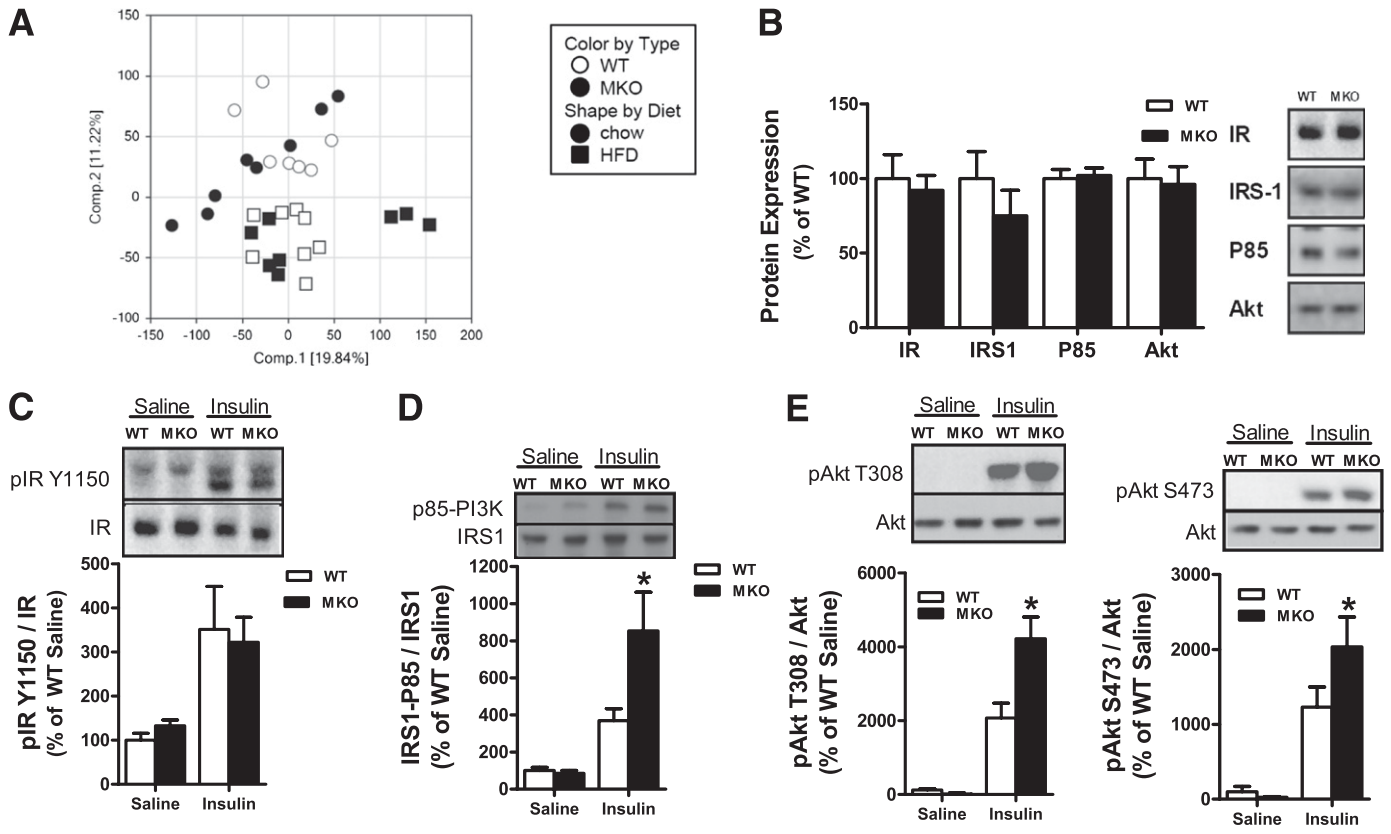

FIG. 5. Increased skeletal muscle IRS1 and Akt phosphorylation in HFD-fed SOCS3 MKO mice. *A*: Principal component analysis of gene expression levels in tibialis anterior muscle from WT and SOCS3 MKO mice fed a chow diet or HFD. A separation between samples can be seen in this visualization (principal component 1 and 2) based on diet (chow = *circles*, HFD = *squares*), but samples are not separated based on genotype (WT = *white*, MKO = *black*). *B*: Skeletal muscle protein expression of the IR, IRS1, P85-subunit of PI3 kinase, and Akt from HFD-fed male WT and SOCS3 MKO mice injected with saline. IR Y1150 phosphorylation (*C*), IRS1-associated P85-subunit of PI3 kinase (*D*), and Akt T308 and S473 phosphorylation (*E*) in HFD-fed male WT and SOCS3 MKO mice injected with either saline or insulin are shown. Data are mean ± SE, n = 6–8. *$P \leq 0.05$ relative to WT.

increase skeletal muscle fatty acid oxidation in lean, but not in obese, rodents (14) and humans (15). Because the overexpression of SOCS3 inhibits leptin-induced activation of both STAT3 and AMPK in skeletal muscle myotubes (17), and because muscle-specific SOCS3 transgenic mice are obese (8), we hypothesized that SOCS3 MKO mice might have increased muscle AMPK, elevated rates of fatty acid oxidation, and increased energy expenditure. However, we found that irrespective of diet, both genotypes increased body weight and adiposity over time to a similar degree. Consistent with this, we found that energy expenditure, activity levels, food intake, mitochondrial capacity, as well as skeletal muscle STAT3 and AMPK phosphorylation were comparable between genotypes. The SOCS3 MKO mice also had similar levels of muscle triglyceride compared with WT littermates. Thus, there is no absolute requirement for skeletal muscle SOCS3 in regulating whole-body energy expenditure in vivo.

The deletion of muscle SOCS3 improved glucose tolerance and insulin sensitivity in obese mice. The development of insulin resistance with obesity is a complex cascade of detrimental events involving several tissue types. We therefore assessed insulin-regulated glucose metabolism using the hyperinsulinemic-euglycemic clamp to determine the relative roles of peripheral tissues (skeletal muscle and adipose tissue) and the liver. Under control chow diet conditions, there were no differences in insulin sensitivity between genotypes. These data suggest that skeletal muscle SOCS3 does not play a major role in regulating insulin-stimulated negative feedback of the insulin signaling pathway (19), which is in contrast to findings in liver-specific SOCS3-null mice (20,21). SOCS3 MKO mice were partially protected against the development of HFD-induced insulin resistance, an effect that was attributable to improved peripheral glucose disposal as a result of enhanced glucose uptake into skeletal muscle, which was assessed both in vivo using PET and ex vivo in isolated skeletal muscle. Thus, deletion of skeletal muscle SOCS3 improves whole-body glucose tolerance and insulin sensitivity in obesity by restoring skeletal muscle insulin sensitivity.

To elucidate the mechanism responsible for muscle insulin sensitization in SOCS3 MKO mice, we performed a genome-wide expression analysis; however, no differences were observed, and thus we also assessed proximal components of the insulin signaling pathway. Previous studies have suggested that SOCS3 antagonizes insulin signaling by blocking phosphorylation of the IRS1 (5). It also has been proposed that SOCS3 can bind to the IR (4,19) or IRS1 (45,46) targeting them for proteolytic degradation and thereby preventing adequate assembling of PI3 kinase complexes. We measured muscle IR expression and Y1150 phosphorylation and found that IR expression and insulin-induced Y1150 phosphorylation were similar between WT and SOCS3 MKO mice. These data suggest that endogenous SOCS3 does not affect either the expression or the phosphorylation of the IR. The IRS1

expression was not altered in SOCS3 MKO mice, but IRS1 tyrosine phosphorylation was increased. Thus, the deletion of SOCS3 enhances IRS1 activation without altering expression levels. Consistent with increased PI3 kinase activation, we found that Akt phosphorylation was enhanced in HFD-fed SOCS3 MKO mice. Therefore, skeletal muscle SOCS3 does not affect the expression of the IR or IRS1, but instead impairs insulin sensitivity by inhibiting the activating phosphorylation of IRS1.

In summary, deletion of SOCS3 in skeletal muscle does not alter muscle contractile performance or the development of obesity but does protect mice from obesity-related glucose intolerance and insulin resistance. Enhanced skeletal muscle insulin sensitivity was attributable to increases in IRS1 activation. Previous studies have shown that liver-specific deletion of SOCS3 promotes lipogenesis, hepatic insulin resistance, and obesity (20,21); however, in the current study we did not detect any detrimental metabolic effects in response to muscle-specific deletion of SOCS3. We conclude that in obesity, muscle SOCS3 is an important contributing factor to muscle insulin resistance and impairments in glucose homeostasis, suggesting that the inhibition of muscle SOCS3 could be a favorable strategy to restore insulin action in patients with type 2 diabetes.

ACKNOWLEDGMENTS

These studies were supported by grants and fellowships from the National Health and Medical Research Council (G.S.L., G.R.S.), Diabetes Australia Research Trust (G.R.S.), the Canadian Foundation for Innovation (G.R.S.), and the Canadian Institutes of Health Research (G.R.S.). S.B.J. was supported by a research fellowship from the Danish Medical Research Council (271-05-0697). M.D.F. is a Canadian Institutes of Health Research Banting Postdoctoral Fellow. J.D.S. is a DeGroote Academic Fellow (McMaster University) and is supported by a Canadian Diabetes Association fellowship. G.R.S. is a Canada Research Chair in Metabolism and Obesity.

S.B.J. is an employee of Novo Nordisk. L.Ö. and A.B. are employees of AstraZeneca. No other potential conflicts of interest relevant to this article were reported.

S.B.J., H.M.O., L.S., J.H., K.A.H., R.P., M.D.F., L.Ö., S.G., C.v.d.P., J.D.S., and G.R.S. researched data. S.B.J., H.M.O., R.P., M.D.F., L.Ö., A.B., S.G., I.A.T., G.S.L., and J.D.S. reviewed and edited the manuscript. G.R.S. designed experiments and wrote the manuscript. G.R.S. is the guarantor of this work and, as such, had full access to all the data in the study and takes responsibility for the integrity of the data and the accuracy of the data analysis.

The authors thank Professors Warren Alexander (Walter and Eliza Hall Institute of Medical Research, University of Melbourne) and C. Ronald Kahn (Joslin Diabetes Center, Harvard Medical School) for providing SOCS3 floxed and muscle creatine kinase promoter mice, respectively. The authors are also grateful for the assistance of Dr. Troy Farncombe and Chantal Saab from the McMaster Centre for Preclinical and Translational Imaging for completing the CT and PET studies, as well as Olga Shyroka (McMaster University) and Timur Naim (University of Melbourne) for providing technical assistance.

REFERENCES

1. Galic S, Oakhill JS, Steinberg GR. Adipose tissue as an endocrine organ. Mol Cell Endocrinol 2010;316:129–139
2. Bjørbaek C, Elmquist JK, Frantz JD, Shoelson SE, Flier JS. Identification of SOCS-3 as a potential mediator of central leptin resistance. Mol Cell 1998; 1:619–625
3. Emanuelli B, Peraldi P, Filloux C, et al. SOCS-3 inhibits insulin signaling and is up-regulated in response to tumor necrosis factor-alpha in the adipose tissue of obese mice. J Biol Chem 2001;276:47944–47949
4. Senn JJ, Klover PJ, Nowak IA, et al. Suppressor of cytokine signaling-3 (SOCS-3), a potential mediator of interleukin-6-dependent insulin resistance in hepatocytes. J Biol Chem 2003;278:13740–13746
5. Ueki K, Kondo T, Kahn CR. Suppressor of cytokine signaling 1 (SOCS-1) and SOCS-3 cause insulin resistance through inhibition of tyrosine phosphorylation of insulin receptor substrate proteins by discrete mechanisms. Mol Cell Biol 2004;24:5434–5446
6. Steinberg GR, Smith AC, Wormald S, Malenfant P, Collier C, Dyck DJ. Endurance training partially reverses dietary-induced leptin resistance in rodent skeletal muscle. Am J Physiol Endocrinol Metab 2004;286:E57–E63
7. Rieusset J, Bouzakri K, Chevillotte E, et al. Suppressor of cytokine signaling 3 expression and insulin resistance in skeletal muscle of obese and type 2 diabetic patients. Diabetes 2004;53:2232–2241
8. Lebrun P, Cognard E, Bellon-Paul R, et al. Constitutive expression of suppressor of cytokine signalling-3 in skeletal muscle leads to reduced mobility and overweight in mice. Diabetologia 2009;52:2201–2212
9. Alexander WS, Hilton DJ. The role of suppressors of cytokine signaling (SOCS) proteins in regulation of the immune response. Annu Rev Immunol 2004;22:503–529
10. Bjorbak C, Lavery HJ, Bates SH, et al. SOCS3 mediates feedback inhibition of the leptin receptor via Tyr985. J Biol Chem 2000;275:40649–40657
11. Kievit P, Howard JK, Badman MK, et al. Enhanced leptin sensitivity and improved glucose homeostasis in mice lacking suppressor of cytokine signaling-3 in POMC-expressing cells. Cell Metab 2006;4:123–132
12. Howard JK, Cave BJ, Oksanen LJ, Tzameli I, Bjørbaek C, Flier JS. Enhanced leptin sensitivity and attenuation of diet-induced obesity in mice with haploinsufficiency of Socs3. Nat Med 2004;10:734–738
13. Mori H, Hanada R, Hanada T, et al. Socs3 deficiency in the brain elevates leptin sensitivity and confers resistance to diet-induced obesity. Nat Med 2004;10:739–743
14. Steinberg GR, Dyck DJ. Development of leptin resistance in rat soleus muscle in response to high-fat diets. Am J Physiol Endocrinol Metab 2000; 279:E1374–E1382
15. Steinberg GR, Parolin ML, Heigenhauser GJ, Dyck DJ. Leptin increases FA oxidation in lean but not obese human skeletal muscle: evidence of peripheral leptin resistance. Am J Physiol Endocrinol Metab 2002;283:E187–E192
16. Steinberg GR, Smith AC, Van Denderen BJW, et al. AMP-activated protein kinase is not down-regulated in human skeletal muscle of obese females. J Clin Endocrinol Metab 2004;89:4575–4580
17. Steinberg GR, McAinch AJ, Chen MB, et al. The suppressor of cytokine signaling 3 inhibits leptin activation of AMP-kinase in cultured skeletal muscle of obese humans. J Clin Endocrinol Metab 2006;91:3592–3597
18. Minokoshi Y, Kim YB, Peroni OD, et al. Leptin stimulates fatty-acid oxidation by activating AMP-activated protein kinase. Nature 2002;415:339–343
19. Emanuelli B, Peraldi P, Filloux C, Sawka-Verhelle D, Hilton D, Van Obberghen E. SOCS-3 is an insulin-induced negative regulator of insulin signaling. J Biol Chem 2000;275:15985–15991
20. Torisu T, Sato N, Yoshiga D, et al. The dual function of hepatic SOCS3 in insulin resistance in vivo. Genes Cells 2007;12:143–154
21. Sachithanandan N, Fam BC, Fynch S, et al. Liver-specific suppressor of cytokine signaling-3 deletion in mice enhances hepatic insulin sensitivity and lipogenesis resulting in fatty liver and obesity. Hepatology 2010;52: 1632–1642
22. Ueki K, Kondo T, Tseng Y-H, Kahn CR. Central role of suppressors of cytokine signaling proteins in hepatic steatosis, insulin resistance, and the metabolic syndrome in the mouse. Proc Natl Acad Sci USA 2004;101: 10422–10427
23. Yaspelkis BB 3rd, Kvasha IA, Figueroa TY. High-fat feeding increases insulin receptor and IRS-1 coimmunoprecipitation with SOCS-3, IKKalpha/beta phosphorylation and decreases PI-3 kinase activity in muscle. Am J Physiol Regul Integr Comp Physiol 2009;296:R1709–R1715
24. Shi H, Cave B, Inouye K, Bjørbaek C, Flier JS. Overexpression of suppressor of cytokine signaling 3 in adipose tissue causes local but not systemic insulin resistance. Diabetes 2006;55:699–707
25. Kiu H, Greenhalgh CJ, Thaus A, et al. Regulation of multiple cytokine signalling pathways by SOCS3 is independent of SOCS2. Growth Factors 2009;27:384–393
26. Brüning JC, Michael MD, Winnay JN, et al. A muscle-specific insulin receptor knockout exhibits features of the metabolic syndrome of NIDDM without altering glucose tolerance. Mol Cell 1998;2:559–569

27. Galic S, Fullerton MD, Schertzer JD, et al. Hematopoietic AMPK β1 reduces mouse adipose tissue macrophage inflammation and insulin resistance in obesity. J Clin Invest 2011;121:4903–4915
28. O'Neill HM, Maarbjerg SJ, Crane JD, et al. AMPK β1β2 muscle null mice reveal an essential role for AMPK in maintaining mitochondrial content and glucose uptake during exercise. Proc Natl Acad Sci USA 2011;108:16092–16097
29. Martin TL, Alquier T, Asakura K, Furukawa N, Preitner F, Kahn BB. Diet-induced obesity alters AMP kinase activity in hypothalamus and skeletal muscle. J Biol Chem 2006;281:18933–18941
30. Dzamko N, van Denderen BJ, Hevener AL, et al. AMPK β1 deletion reduces appetite, preventing obesity and hepatic insulin resistance. J Biol Chem 2010;285:115–122
31. Schertzer JD, Gehrig SM, Ryall JG, Lynch GS. Modulation of insulin-like growth factor (IGF)-I and IGF-binding protein interactions enhances skeletal muscle regeneration and ameliorates the dystrophic pathology in mdx mice. Am J Pathol 2007;171:1180–1188
32. Jørgensen SB, Honeyman J, Oakhill JS, et al. Oligomeric resistin impairs insulin and AICAR-stimulated glucose uptake in mouse skeletal muscle by inhibiting GLUT4 translocation. Am J Physiol Endocrinol Metab 2009;297: E57–E66
33. Saab C, Labiris N, Chirakal R, Farncombe T. A database of normal PET and SPECT radiotracer distributions in rats and mice. J Nucl Med Meeting Abstracts 2007;48:292P-b.
34. Watt MJ, Dzamko N, Thomas WG, et al. CNTF reverses obesity-induced insulin resistance by activating skeletal muscle AMPK. Nat Med 2006;12:541–548
35. Beck Jørgensen S, O'Neill HM, Hewitt K, Kemp BE, Steinberg GR. Reduced AMP-activated protein kinase activity in mouse skeletal muscle does not exacerbate the development of insulin resistance with obesity. Diabetologia 2009;52:2395–2404
36. Trounce IA, Kim YL, Jun AS, Wallace DC. Assessment of mitochondrial oxidative phosphorylation in patient muscle biopsies, lymphoblasts, and transmitochondrial cell lines. Methods Enzymol 1996;264:484–509
37. Spangenburg EE. SOCS-3 induces myoblast differentiation. J Biol Chem 2005;280:10749–10758
38. Corpeleijn E, Saris WH, Blaak EE. Metabolic flexibility in the development of insulin resistance and type 2 diabetes: effects of lifestyle. Obes Rev 2009;10:178–193
39. Buettner C, Muse ED, Cheng A, et al. Leptin controls adipose tissue lipogenesis via central, STAT3-independent mechanisms. Nat Med 2008;14: 667–675
40. Jørgensen SB, Treebak JT, Viollet B, et al. Role of AMPKalpha2 in basal, training-, and AICAR-induced GLUT4, hexokinase II, and mitochondrial protein expression in mouse muscle. Am J Physiol Endocrinol Metab 2007; 292:E331–E339
41. Winder WW, Holmes BF, Rubink DS, Jensen EB, Chen M, Holloszy JO. Activation of AMP-activated protein kinase increases mitochondrial enzymes in skeletal muscle. J Appl Physiol 2000;88:2219–2226
42. Li L, Pan R, Li R, et al. Mitochondrial biogenesis and peroxisome proliferator-activated receptor-γ coactivator-1α (PGC-1α) deacetylation by physical activity: intact adipocytokine signaling is required. Diabetes 2011; 60:157–167
43. Savage DB, Petersen KF, Shulman GI. Disordered lipid metabolism and the pathogenesis of insulin resistance. Physiol Rev 2007;87:507–520
44. Iyer A, Fairlie DP, Prins JB, Hammock BD, Brown L. Inflammatory lipid mediators in adipocyte function and obesity. Nat Rev Endocrinol 6:71-82
45. Rui L, Yuan M, Frantz D, Shoelson S, White MF. SOCS-1 and SOCS-3 block insulin signaling by ubiquitin-mediated degradation of IRS1 and IRS2. J Biol Chem 2002;277:42394–42398
46. Shi H, Tzameli I, Bjørbaek C, Flier JS. Suppressor of cytokine signaling 3 is a physiological regulator of adipocyte insulin signaling. J Biol Chem 2004; 279:34733–34740
47. Tartaglia LA, Dembski M, Weng X, et al. Identification and expression cloning of a leptin receptor, OB-R. Cell 1995;83:1263–1271